Electronic Supplementary Information

Crystal-to-Crystal Polymerisation of Monosubstituted $[PW_{11}O_{39}Cu(H_2O)]^{5-}$ Keggin-Type Anions

Estibaliz Ruiz-Bilbao,[a,b] Aroa Pache,[a] Unai Barrenechea,[a] Santiago Reinoso,[c] Leire San Felices,[d] Maria dM. Vivanco,[e] Luis Lezama,[a] Beñat Artetxe,[*a] and Juan M. Gutiérrez-Zorrilla[*a,b]

[a] Departamento de Química Orgánica e Inorgánica, Facultad de Ciencia y Tecnología, Universidad del País Vasco UPV/EHU, P.O. Box 644, 48080 Bilbao, Spain.

[b] BCMaterials Edificio Martina Casiano, 3rd Floor, UPV/EHU Science Park, Barrio Sarriena s/n, 48940 Leioa, Spain.

[c] Institute for Advanced Materials and Mathematics (INAMAT2), Departamento de Ciencias, Universidad Pública de Navarra (UPNA), Campus de Arrosadia, 31006 Pamplona, Spain.

[d] Servicios Generales de Investigación SGIker, Facultad de Ciencia y Tecnología, Universidad del País Vasco UPV/EHU P.O. Box 644, 48080 Bilbao, Spain.

[e] Cancer Heterogeneity Lab, Center for Cooperative Research in Biosciences (CIC bioGUNE), Basque Research and Technology Alliance (BRTA), Bizkaia Technology Park, 48160 Derio, Spain.

TABLE OF CONTENTS .....

FIGURES

EQUATIONS

TABLES

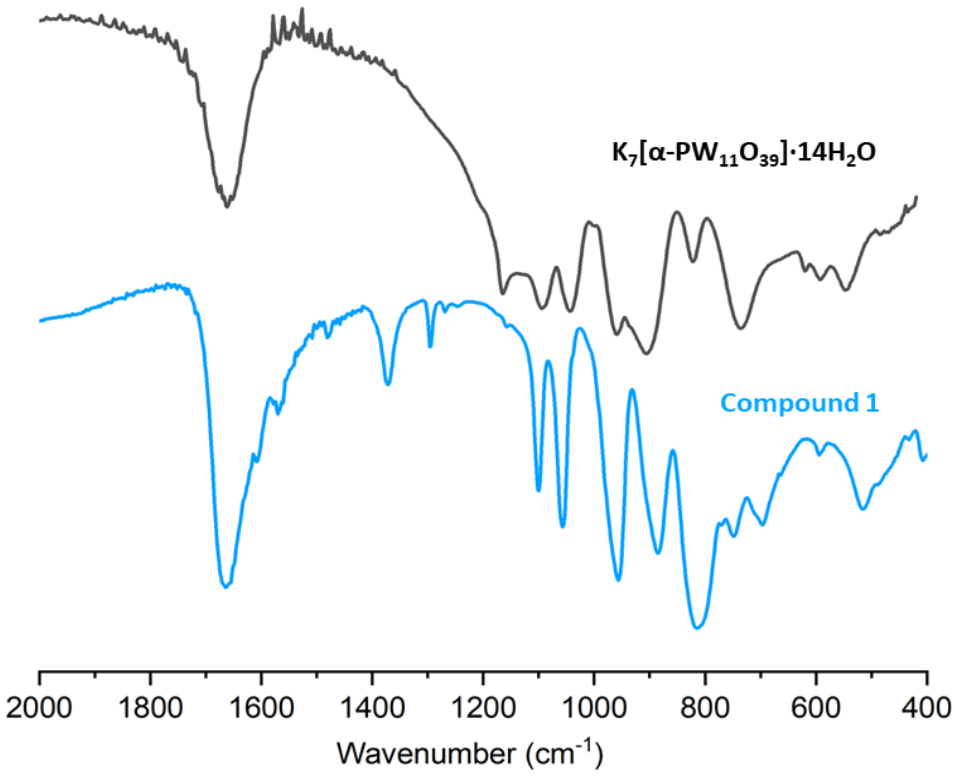

Figure S1. FTIR spectrum of **1** (blue) compared to that of the $K_7[\alpha\text{-}PW_{11}O_{39}]\cdot 14H_2O$ precursor.

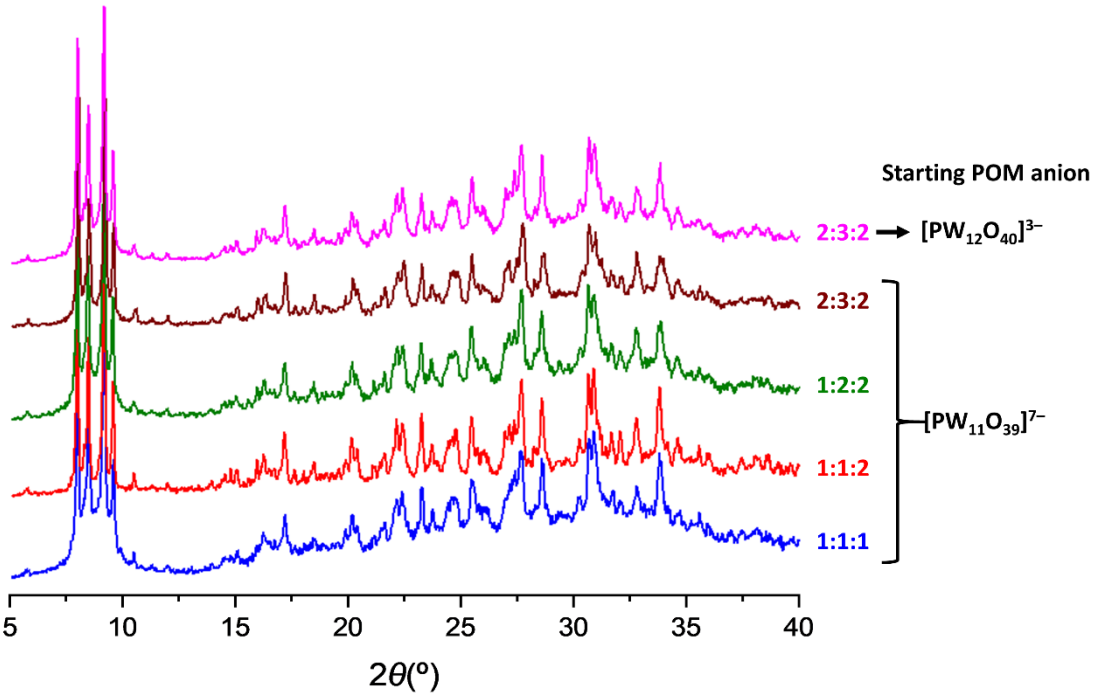

Figure S2. PXRD diffraction patterns for the syntheses carried out for different POM:Cu^{2+}:pic ratios.

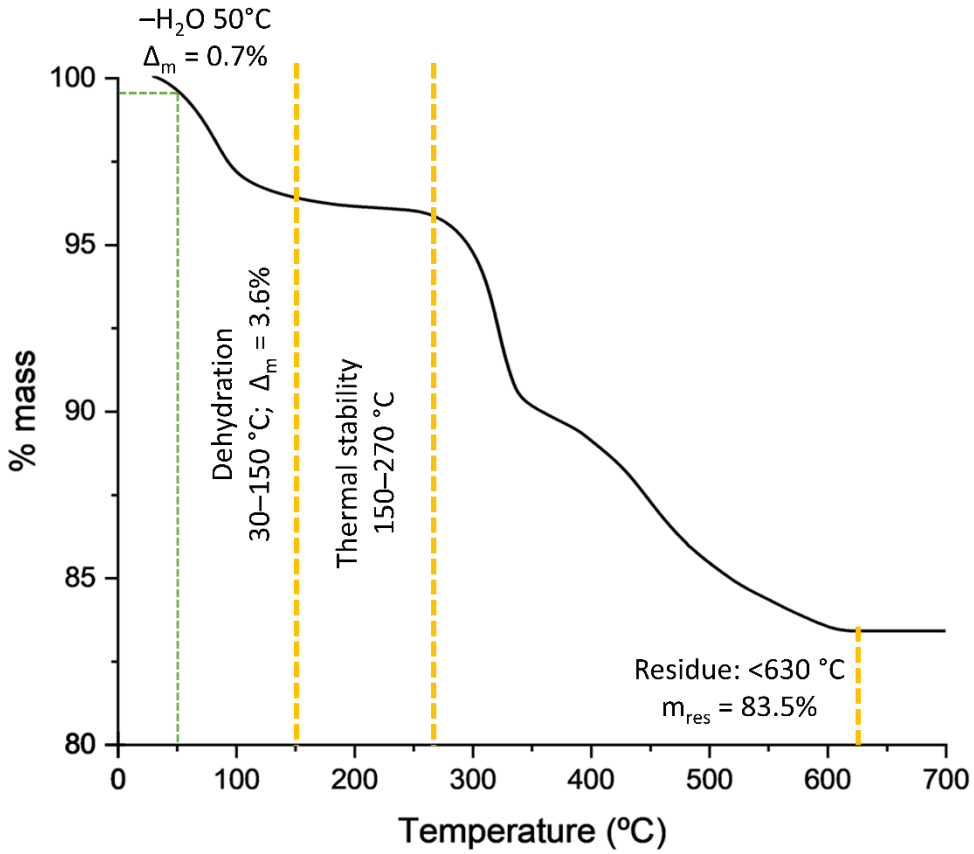

Figure S3. TGA curve for **1**.

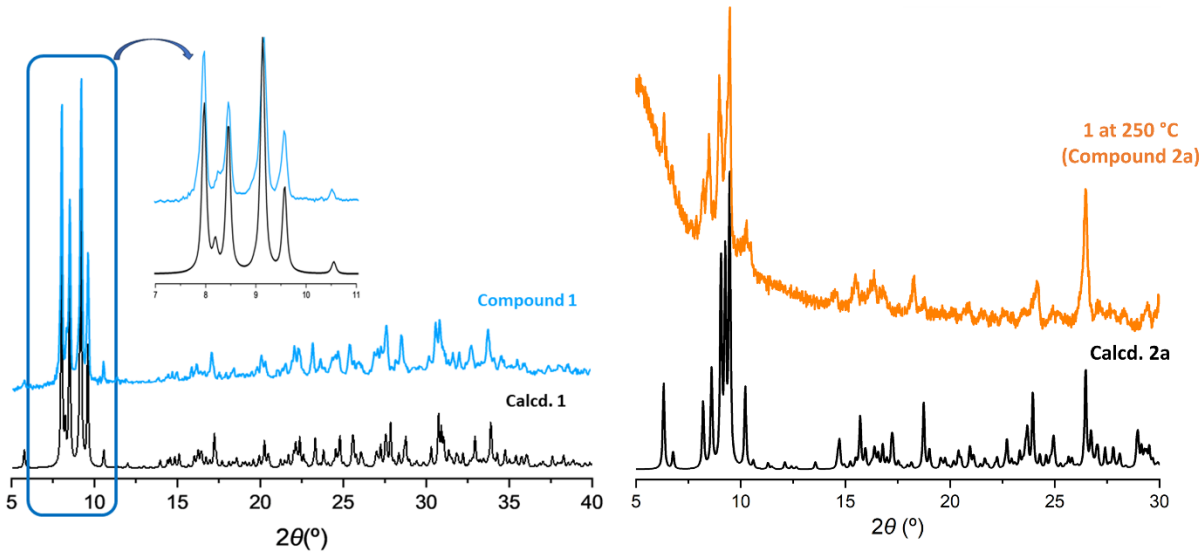

Figure S4. Comparison of the PXRD patterns collected for **1** at room temperature and 250 °C with those calculated from SCXRD data for **1** and **2a**, respectively.

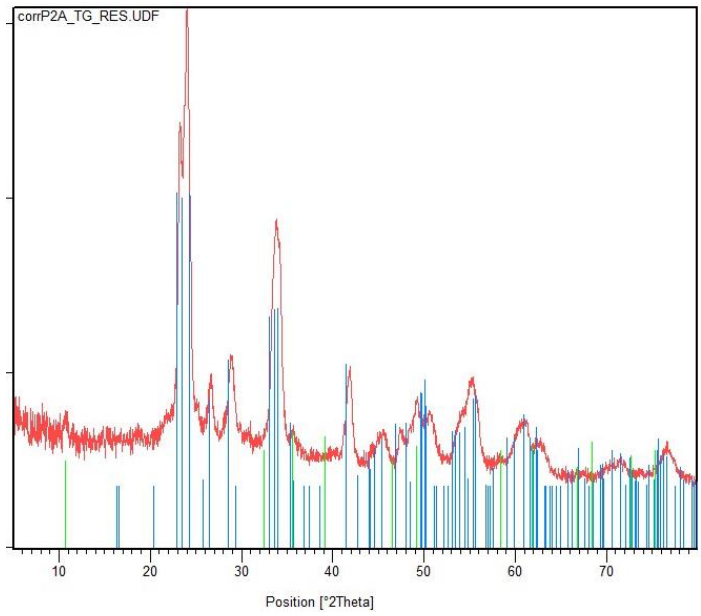

Figure S5. Identification of the final residue from the thermal decomposition of **1** by PXRD analyses. Blue lines correspond to diffraction maxima from monoclinic *Pmnb* WO_3 (PDF: 01-071-0131) and green lines to monoclinic *C*2/*c* CuO (PDF: 00-002-1041).

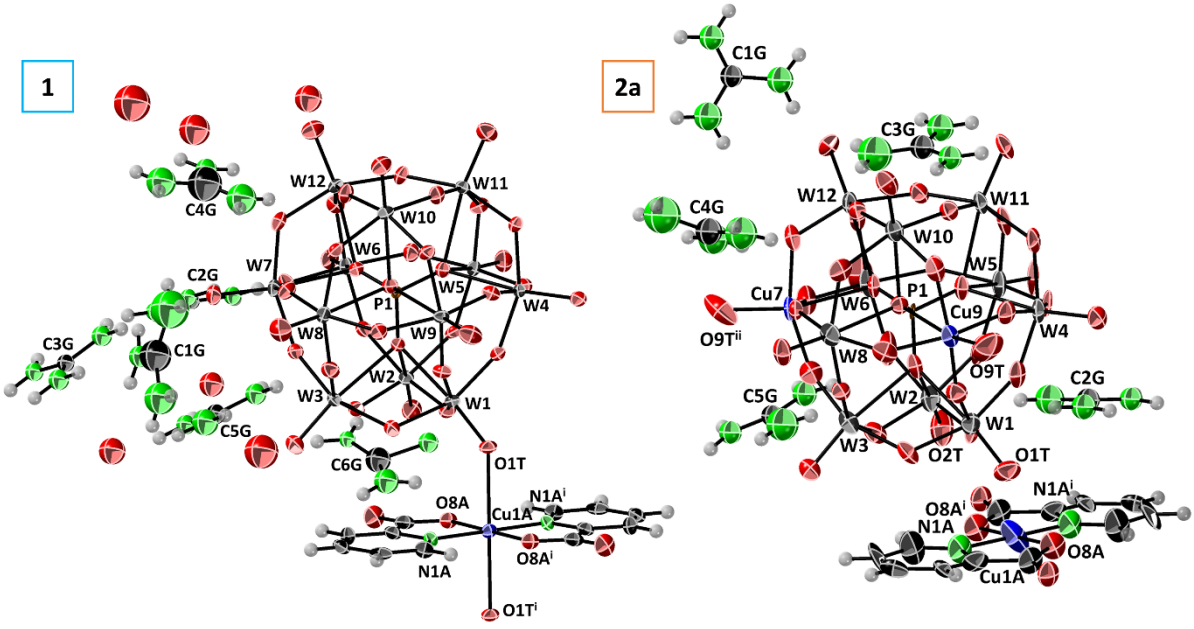

Figure S6. ORTEP representation of **1** and **2a** showing 50% probability ellipsoids and atom labelling scheme. Colour code: Mo, grey; P, dark red; Cu, blue; O, red; N, green; C, black; H, light grey. The disordered Cu^{II} atom in the Keggin anion has been omitted for **1**, but has been depicted on the addenda metal positions 7 and 9 for **2a**. Symmetry codes: i) –x, -y, 1-z; ii) 1-x, ½+y, ½-z.

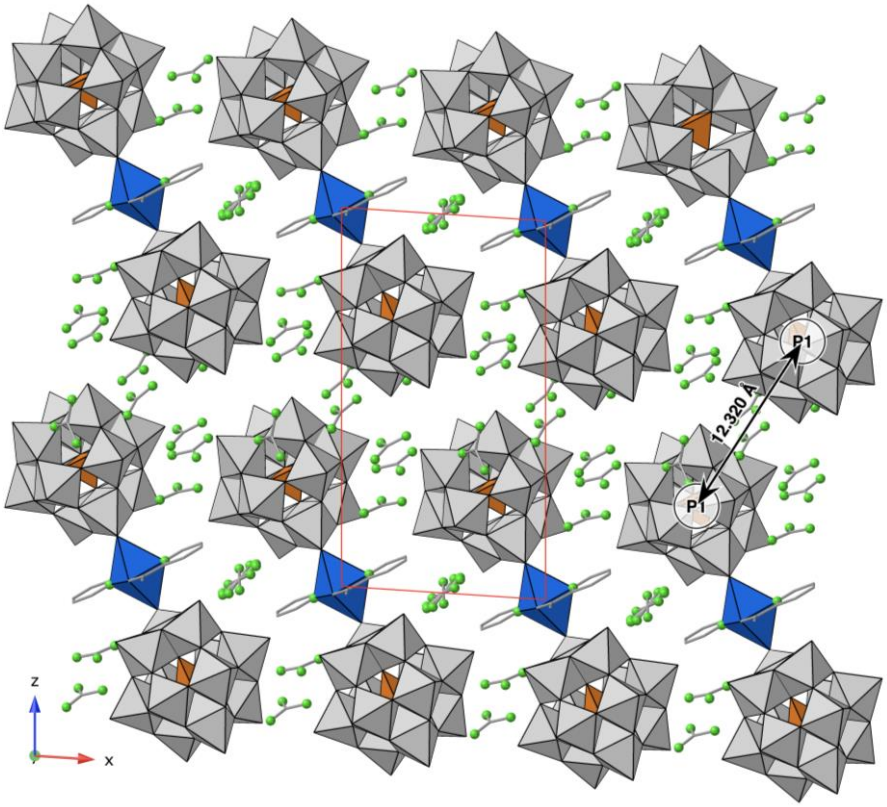

Figure S7. View of the crystal packing of **1** along the crystallographic y axis.

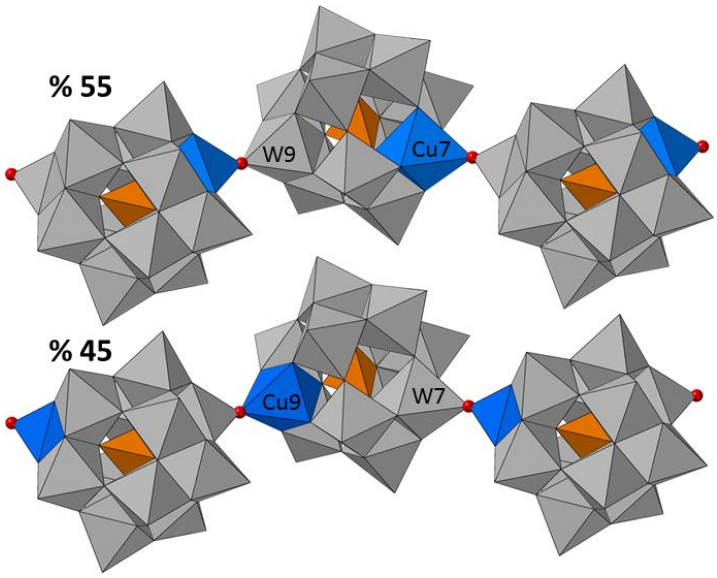

Figure S8. Polyhedral representation of $\{PW_{11}O_{39}Cu\}_n$ chains in **2a**.

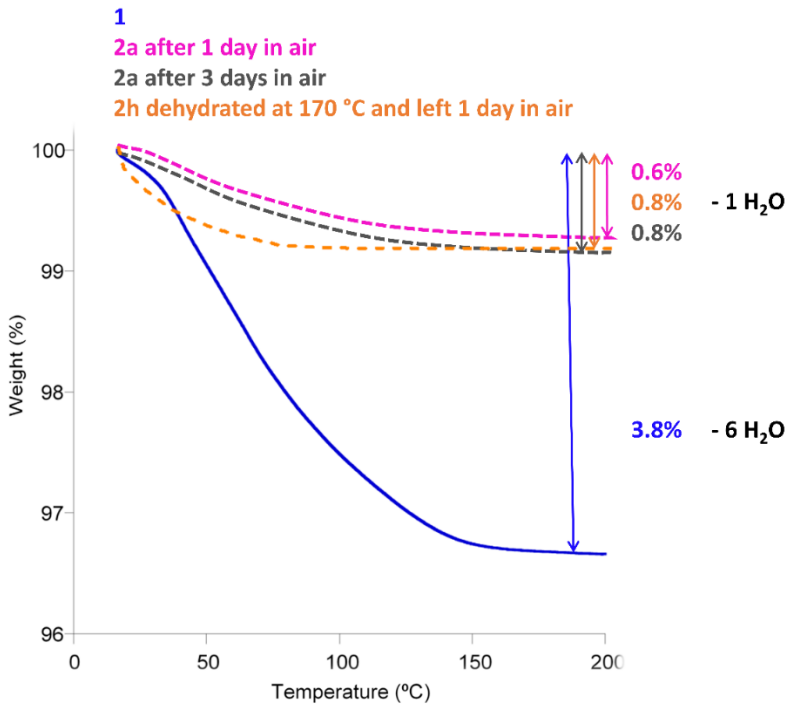

Figure S9. TGA curve for the dehydration of **1** (blue) compared to those of samples of **2a** left to hydrate in open air for 1 (pink) or 3 days (grey), as well as that of **2h** dehydrated at 170 °C and exposed to ambient moisture for 1 day (orange).

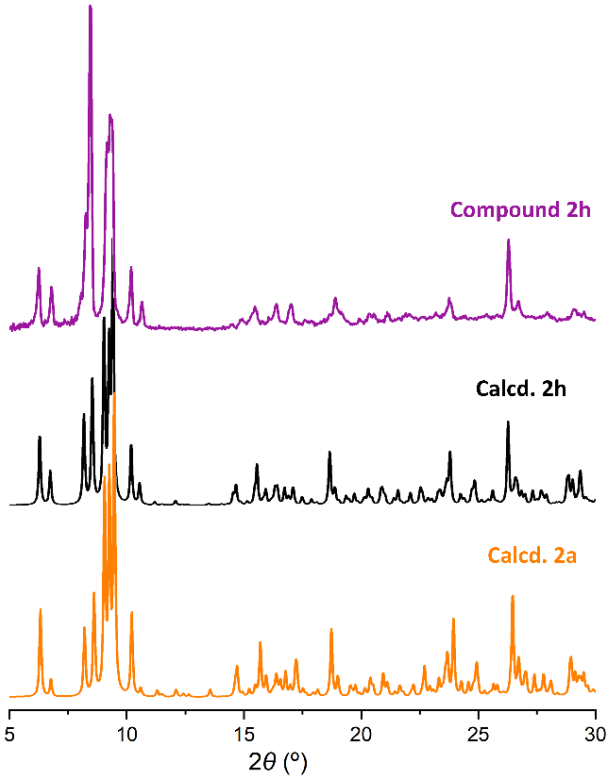

Figure S10. Experimental PXRD pattern of **2h** prepared by exposing crystals of **2a** to room atmosphere for one day compared to those calculated from scXRD data for **2a** and **2h**.

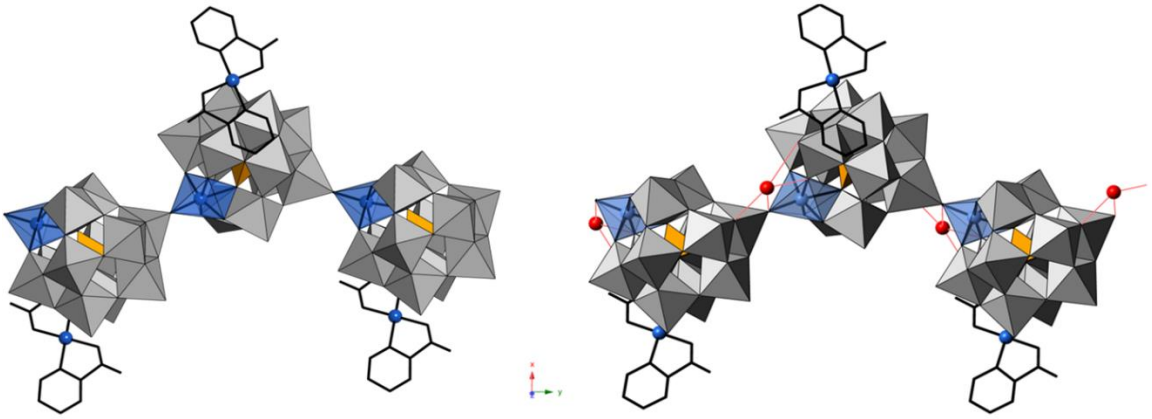

Figure S11. Structural comparison of the polymeric entities in **2a** (left) and **2h** (right). Hydrogen-bonding interactions involving water molecules are depicted as red lines.

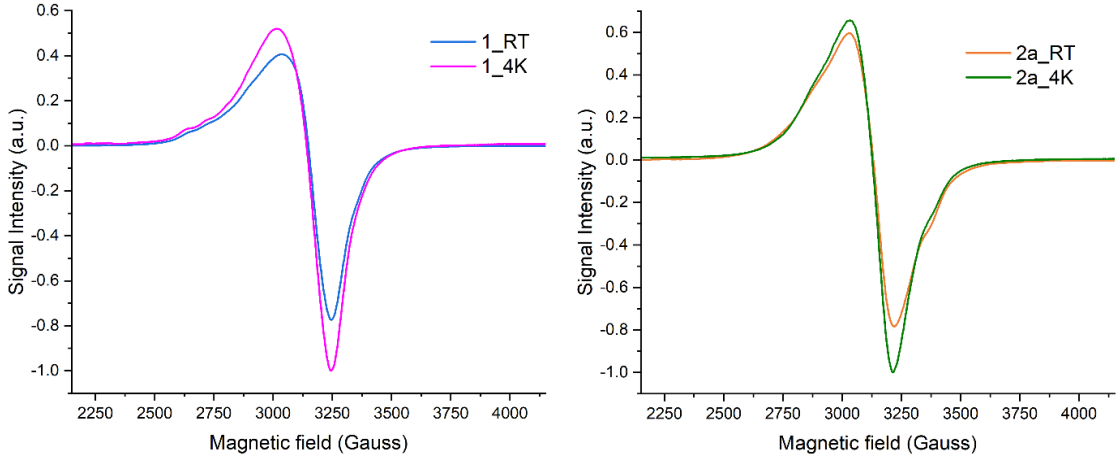

Figure S12. X-band EPR spectra at room temperature and 4K for **1** (left) and **2a** (right).

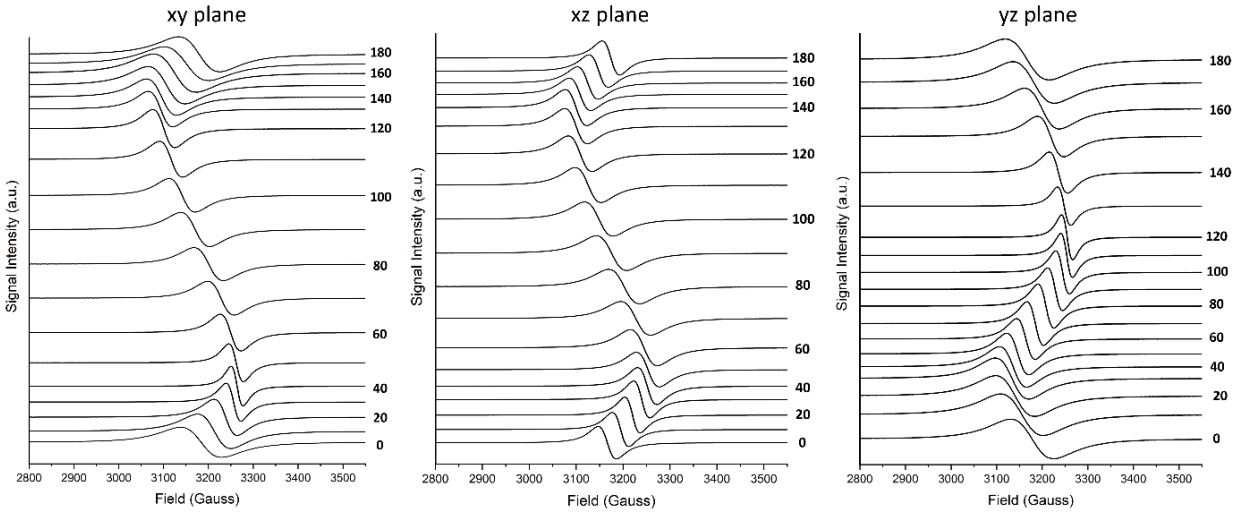

Figure S13. Evolution of the X-band EPR single-crystal spectra of **1** for the three perpendicular xy, xz and yz planes. The spectra were recorded for different angles every 10°.

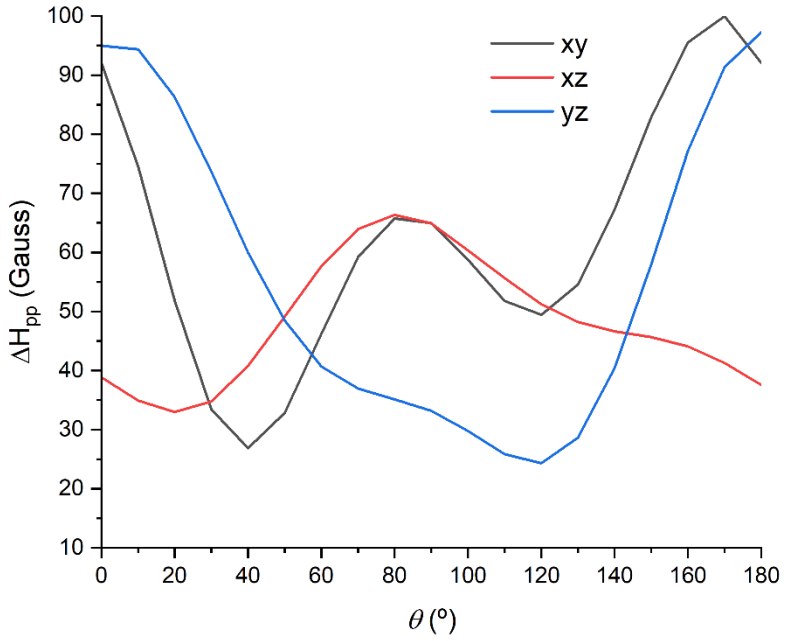

Figure S14. Angular variation of the linewidth in X-band EPR single-crystal spectra of **1** for the xy, xz and yz planes.

Equation 1. Set of equations employed to fit the angular variation of the EPR signal in three mutually perpendicular planes. The principal g values were calculated by diagonalization of the obtained g^2 tensor.

$$g^2_{(xy)} = g_{xx}^2 \cos^2(\theta) + 2\, g_{xy} \cos(\theta) \sin(\theta) + g_{yy}^2 \sin^2(\theta)$$

$$g^2_{(xz)} = g_{xx}^2 \cos^2(\theta) + 2\, g_{xz} \cos(\theta) \sin(\theta) + g_{zz}^2 \sin^2(\theta)$$

$$g^2_{(yz)} = g_{yy}^2 \cos^2(\theta) + 2\, g_{yz} \cos(\theta) \sin(\theta) + g_{zz}^2 \sin^2(\theta)$$

Table S1. Copper population factors for the addenda metal positions within the inorganic $[PW_{11}O_{39}Cu(H_2O)]^{5-}$ building-block in **1**, **2a** and **2h**.

	W1	W2	W3	W4	W5	W6	W7	W8	W9	W10	W11	W12
1	–	4.8	7.9	9.0	7.9	3.2	10.6	18.6	18.5	4.2	6.9	8.4
2a	–	–	–	–	–	–	44.9	–	55.1	–	–	–
2h	–	–	–	–	–	–	45.0	–	55.0	–	–	–

Table S2. Cu–O and Cu–N bond lengths (Å) and O–Cu–N and O–Cu–O angles (°) in the metalorganic units of **1**, **2a** and **2h**.

1		**2a**		**2h**	
Cu1A–O1T	2.507(5)	Cu1A···O2T	3.79(3)	Cu1A–O2T	3.99(3)
Cu1A–O1T^{i}	2.507(5)	Cu1A···O2T^{i}	3.79(3)	Cu1A–O2T^{i}	3.99(3)
Cu1A–O8A	1.945(5)	Cu1A–O8A	1.91(2)	Cu1A–O8A	1.89(3)
Cu1A–O8A^{i}	1.945(5)	Cu1A–O8A^{i}	1.91(2)	Cu1A–O8A^{i}	1.89(3)
Cu1A–N1A	1.951(7)	Cu1A–N1A	1.99(4)	Cu1A–N1A	1.87(4)
Cu1A–N1A^{i}	1.951(7)	Cu1A–N1A^{i}	1.99(4)	Cu1A–N1A^{i}	1.87(4)

Symmetry code: i)1 -x, 1-y, 1-z.

Table S3. Geometrical parameters of the intermolecular N–H···O and C–H···O hydrogen bonds in **1**, **2a** and **2h**.

Donor–H···Acceptor	**D–H**	**H···A**	**D···A**	**D–H···A**
1				
N1G–H1GA···O3W^{i}	0.88	1.93	2.743(18)	153
N1G–H1GB···O1W	0.88	2.03	2.889(17)	167
N2G–H2GA···O910^{ii}	0.88	2.42	3.127(11)	138
N2G–H2GB···O2W^{iii}	0.88	2.19	3.065(14)	174
N3G–H3GB···O2T	0.88	2.48	3.278(18)	152
N4G–H4GA···O910^{iv}	0.88	2.05	2.920(9)	170
N4G–H4GB···O67	0.88	2.18	3.030(91)	163
N5G–H5GA···O12^{ii}	0.88	2.49	3.326(9)	159
N5G–H5GB···O810^{iv}	0.88	2.16	3.030(9)	168
N10G–H10B···O712^{v}	0.88	2.24	2.926(16)	135
N10G–H10A···O5W	0.88	2.14	2.85(2)	137
N6G–H6GA···O14^{ii}	0.88	2.17	2.953(9)	148
N6G–H6GB···O6T	0.88	2.25	3.043(9)	150
N7G–H7GA···O9A	0.88	2.36	3.024(10)	133
N13G–H13A···O4T^{ii}	0.88	2.19	3.040(10)	163
N13G–H13B···O37	0.88	2.29	3.096(11)	151
N14G–H14A···O45^{ii}	0.88	2.05	2.912(10)	167
N14G–H14B···O11T^{i}	0.88	2.35	3.077(11)	140
N8G–H8GB···O9A	0.88	2.08	2.820(9)	141
N15G–H15A···O2W^{ii}	0.88	2.15	3.011(14)	165
N15G–H15B···O3T	0.88	2.45	3.194(11)	143
N8G–H8GB···O56^{i}	0.88	2.49	3.103(11)	127
N9G–H9GA···O411^{ii}	0.88	2.04	2.906(8)	168
N9G–H9GB···O511^{i}	0.88	2.12	2.961(8)	160
C3A–H3A···O89^{vi}	0.95	2.28	3.212(11)	166
C5A–H5A···O612^{i}	0.95	2.33	3.043(11)	131

Table S3 (continuation). Geometrical parameters of the intermolecular N–H···O and C–H···O type hydrogen bonds in **1**, **2a** and **2h**.

2a				
N1G–H1GA···O9A^{vii}	0.88	2.12	2.87(3)	143
N2G–H2GA···O910^{viii}	0.88	2.07	2.89(3)	155
N2G–H2GB···O12T	0.88	2.07	2.85(3)	148
N3G–H3GA···O9A^{vii}	0.88	2.11	2.87(3)	144
N3G–H3GB···O49^{viii}	0.88	2.46	3.17(3)	138
N4G–H4GA···O67^{ix}	0.88	2.12	2.95(3)	159
N4G–H4GB···O89^{x}	0.88	2.08	2.95(3)	168
N5G–H5GA···O8T^{x}	0.88	1.88	2.75(3)	172
N5G–H5GB···O2T	0.88	2.31	3.11(4)	151
N5G–H5GB···O25	0.88	2.25	2.93(3)	134
N10G–H10A···O78	0.88	2.33	3.07(3)	142
N6G–H6GA···O6T^{ix}	0.88	1.93	2.80(3)	171
N11G–H11A···O6T^{xi}	0.87	2.51	3.13(4)	129
N11G–H11B···O1T^{vii}	0.88	2.26	3.05(4)	149
N6G–H6GB···O14	0.89	2.58	3.27(3)	135
N12G–H12A···O810	0.88	2.15	3.01(4)	168
N12G–H12B···O5T0^{xi}	0.88	2.21	2.96(4)	144
N7G–H7GA···O9A^{xii}	0.88	1.97	2.81(3)	159
N13G–H13B···O45^{xii}	0.88	2.05	2.91(3)	165
N7G–H7GB···O411^{xiii}	0.88	1.96	2.80(3)	161
N14G–H14A···O10T^{vii}	0.88	2.29	3.09(3)	152
N14G–H14B···O5T^{xii}	0.88	2.03	2.90(3)	171
N8G–H8GA···O8A^{xii}	0.87	2.36	3.20(4)	161
N15G–H15A···O23	0.88	2.19	2.98(4)	150
N15G–H15B···O12T^{i}	0.88	2.18	2.91(4)	139
N8G–H8GB···O612	0.88	2.13	2.95(4)	154
2h				
N1G–H1GA···O9^{xiv}	0.88	1.99	2.78(5)	149
N1G–H1GB···O1W^{xiv}	0.88	1.91	2.70(6)	150
N2–H2A···O45^{xii}	0.88	2.05	2.92(4)	172
N2G–H2GA···O12T^{viii}	0.87	2.22	2.98(5)	147
N3–H3A···O10T^{vii}	0.87	2.27	3.11(3)	161
N3–H3B···O5T^{xii}	0.88	2.21	2.97(4)	160
N2G–H2GB···O910	0.88	2.12	2.94(4)	154
N3G–H3GA···O9^{xiv}	0.88	2.35	3.04(5)	136
N3G–H3GB···O49	0.88	2.32	3.06(4)	141
N4G–H4GA···O89^{xv}	0.88	2.08	2.94(3)	169
N4G–H4GB···O67^{ix}	0.88	2.14	2.98(3)	160
N5G–H5GA···O2T	0.88	2.47	3.25(5)	150
N5G–H5GA···O25	0.88	2.25	2.95(4)	137
N5G–H5GB···O8T^{xv}	0.88	1.89	2.77(4)	172
N10G–H10A···O8T^{xv}	0.87	2.36	3.05(10)	136
N10G–H10B···O4T^{xii}	0.89	2.50	3.23(9)	139
N6G–H6GA···O14	0.88	2.59	3.26(4)	134
N11G–H11A···O11T^{xiii}	0.87	2.12	2.98(8)	170
N6G–H6GB···O6T^{ix}	0.88	2.01	2.87(4)	168
N7G–H7GA···O411^{xiii}	0.88	2.01	2.84(4)	156
N13G–H13A···O4T^{xii}	0.88	2.31	3.11(8)	151
N7G–H7GA···O9^{xii}	0.88	1.99	2.83(4)	160
N14G–H14B···O6T	0.87	2.38	3.13(8)	145
N8G–H8GA···O612	0.88	2.15	3.00(5)	163
N15G–H15A···O12T^{i}	0.88	2.36	3.01(5)	132
N15G–H15B···O23	0.88	2.33	3.08(4)	143
N8G–H8GB···O8^{xii}	0.87	2.34	3.20(5)	167

Symmetry codes: i) x, ½-y, ½+z; ii) 1-x, -½+y, ½-z;iii) -x, -1/2+y, ½-z; iv) 2-x, -1/2+y, ½-z; v) -1+x, y, z; vi) 2-x, 1-y, 1-z; vii) 1-x, ½+y, ½-z; viii) 1-x, -y, -z; ix) -x, -1/2+y, ½-z; x) -1+x, y, z; xi) 1+x, y, z; xii) -x, ½+y, ½-z; xiii) -x, -y, -z; xiv) x, -1/2-y, -1/2+z; xv) 1+x, y, z.

Table S4 Distances (Å) from the O atoms of W1-W2-W3 trimers to picolinate ring centroids in **2a** and **2h** (Cg_{pic} = N1A, C2A, C3A, C4A, C5A, C6A).

	2a	**2h**
O1T···Cg_{pic}	3.70(2)	3.63(3)
O2T···Cg_{pic}	4.97(2)	5.16(3)
O3T···Cg_{pic}	4.13(3)	4.17(2)
O12···Cg_{pic}	3.79(2)	3.87(2)
O13···Cg_{pic}	3.23(2)	3.26(2)
O23···Cg_{pic}	3.98(2)	4.13(2)

Table S5. Distances (Å) from the O atoms of W1-W2-W3 trimers to picolinate ring planes (N1A, C2A, C3A, C4A, C5A, C6A) in **2a** and **2h**

	2a	**2h**
O1T···plane	2.724	2.864
O2T···plane	2.676	2.728
O3T···plane	2.613	2.475
O12···plane	3.212	3.357
O13···plane	3.159	3.170
O23···plane	3.109	3.100